#### LETTER TO THE EDITOR

# Unidentified quasars among stationary objects from Gaia DR2

K. E. Heintz<sup>1,2</sup>, J. P. U. Fynbo<sup>2</sup>, E. Høg<sup>3</sup>, P. Møller<sup>4</sup>, J.-K. Krogager<sup>5</sup>, S. Geier<sup>6,7</sup>, P. Jakobsson<sup>1</sup> and L. Christensen<sup>8</sup>

- Centre for Astrophysics and Cosmology, Science Institute, University of Iceland, Dunhagi 5, 107 Reykjavík, Iceland
- The Cosmic Dawn Center, Niels Bohr Institute, University of Copenhagen, Juliane Maries Vej 30, 2100 Copenhagen Ø, Denmark
- Niels Bohr Institute, University of Copenhagen, Juliane Maries Vej 30, 2100 Copenhagen Ø, Denmark
- European Southern Observatory, Karl-Schwarzschildstrasse 2, D-85748 Garching bei München, Germany
- Institut d'Astrophysique de Paris, CNRS-UPMC, UMR7095, 98bis bd Arago, 75014 Paris, France
- Gran Telescopio Canarias (GRANTECAN), Cuesta de San José s/n, E-38712, Breña Baja, La Palma, Spain
- Instituto de Astrofísica de Canarias, Vía Láctea s/n, E38200, La Laguna, Tenerife, Spain
- Dark Cosmology Centre, Niels Bohr Institute, University of Copenhagen, Juliane Maries Vej 30, 2100 Copenhagen Ø, Denmark

#### **ABSTRACT**

Furopean Southern Observatory, Karl-Schwarzschildstrasse 2, E Institut d'Astrophysique de Paris, CNRS-UPMC, UMR7095, 98
G Gran Telescopio Canarias (GRANTECAN), Cuesta de San José
Instituto de Astrofísica de Canarias, Vía Láctea s/n, E38200, La
Dark Cosmology Centre, Niels Bohr Institute, University of Cop
Received 2018; accepted 2018

ABST

We here apply a novel technique selecting quasar candidates pure (DR2). We demonstrate that this approach is highly efficient towa sources. Such a selection technique offers a very pure sample cogardless of their intrinsic spectral properties within the limiting mucompiled by including all Gaiα-DR2 sources within one degree oconsistent with zero within 2σ uncertainty. By cross-matching the mid-infrared AllWISE photometric catalogues we investigate the consistent with zero within 2σ uncertainty. By cross-matching the mid-infrared values are therefore able to determine the elesources, but some may also be quasars with colours similar to stan ended to unveil such a hitherto hidden quasar population. This important questions concerning quasars such as determining the fine (BAL) quasars, and the metallicity distribution of damped Lytypes of quasars or even new classes of cosmological point sources (Key words. astrometry – proper motions – general: quasars

1. Introduction

There is great interest in building unbiased catalogues of quasars for a range of important astrophysical questions. These include understanding the quasar phenomenon itself and the growth and occurrence of supermassive black holes through cosmic time, the use of quasars as probes of intervening material and their role in in re-ionisation of both hydrogen and helium, and for the UV background levels throughout the universe (Hewett & Foltz 1994; Weymann et al. 1981). Most current quasar surveys, however, rely on their specific intrinsic properties such as strong ultraviolet emission (Schneider et al. 2010), distinct near/midinfrared colours (Maddox et al. 2012; Secrest et al. 2015), X-ray We here apply a novel technique selecting quasar candidates purely as sources with zero proper motions in the Gaia data release 2 (DR2). We demonstrate that this approach is highly efficient toward high Galactic latitudes with ≤ 25% contamination from stellar sources. Such a selection technique offers a very pure sample completeness, since all cosmological point sources are selected regardless of their intrinsic spectral properties within the limiting magnitude of Gaia. We carry out a pilot-study by defining a sample compiled by including all Gaia-DR2 sources within one degree of the North Galactic Pole (NGP) selected to have proper motions consistent with zero within  $2\sigma$  uncertainty. By cross-matching the sample to the optical Sloan Digital Sky Survey (SDSS) and the mid-infrared AllWISE photometric catalogues we investigate the colours of each of our sources. Together with already spectroscopically confirmed quasars we are therefore able to determine the efficiency of our selection. The majority of the zero proper motion sources have optical to mid-infrared colours consistent with known quasars. The remaining population may be contaminating stellar sources, but some may also be quasars with colours similar to stars. Spectroscopic follow-up of the zero proper motion sources is needed to unveil such a hitherto hidden quasar population. This approach has the potential to allow substantial progress on many important questions concerning quasars such as determining the fraction of dust-obscured quasars, the fraction of broad absorption line (BAL) quasars, and the metallicity distribution of damped Lyman- $\alpha$  absorbers. The technique could also potentially reveal new types of quasars or even new classes of cosmological point sources.

ultraviolet emission (Schneider et al. 2010), distinct near/midinfrared colours (Maddox et al. 2012; Secrest et al. 2015), X-ray output (Brusa et al. 2010) or prominent radio emission (Ivezić et al. 2002).

In this Letter we apply an astrometric approach of identifying quasars as apparently stationary sources on the sky, based purely on the astrometric measurement from the Gaia mission (Heintz et al. 2015), and present the first pilot study of such an approach. Our goal here is to quantify the efficiency and completeness of this selection technique. Identifying quasars based only on their zero proper motions has the potential to open a novel route of selecting quasars in an unbiased way, and might even lead to the discovery of new types of quasars or other types of extragalactic point sources.

#### 2. Astrometric selection of quasars

The Gaia data release 2 (DR2; Gaia Collaboration et al. 2018) catalogue consists of more than  $1.3 \times 10^9$  sources down to  $G \approx 21$ mag, for which the five-parameter astrometric solution (positions, parallaxes and proper motions) has been determined (Lindegren et al. 2018). The Gaia G filter is very broad covering the spectral range from 400 to 1000 nm and hence quasars covering a wide range of redshifts should be included in the catalogue.

We extract all sources within a radius of one degree from the North Galactic Pole (NGP) centred on  $(\alpha, \delta) = 12^{\rm h} 51^{\rm m} 26^{\rm s}.0 +$ 27° 07<sup>m</sup> 42<sup>s</sup>.0 from the *Gaia* DR2 catalogue (see Fig. 1). We then limit our search to sources with 18 < G < 20 mag, for which the associated uncertainty is up to 1.2 mas yr<sup>-1</sup> in the respective proper motion components. This is motivated by our pre-study (Heintz et al. 2015) in which we (based on pre-launch simulations of the Gaia-data) found that the expected contamination of apparently stationary stars is lower than  $\approx 20\%$  at the Galactic poles, but increases significantly when observing closer to the Galactic plane or at magnitudes brighter than G < 18mag. We then select all point sources with total proper motions,

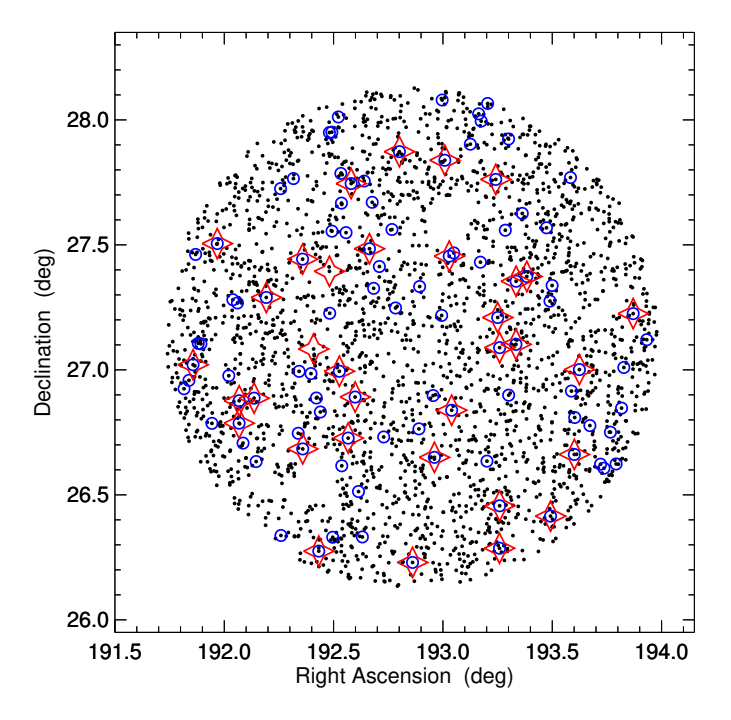


**Fig. 1.** Location on the sky of all point-like *Gaia* sources with proper motions and 18 < G < 20 mag (black dots) within one degree of the NGP. The subset of these with proper motions consistent with zero within  $2\sigma$  are shown by the blue circles and those that are already spectroscopically confirmed quasars are shown by the red star symbols.

 $\mu = \sqrt{\mu_{\rm RA}^2 + \mu_{\rm Dec}^2}$ , consistent with zero at the  $2\sigma$  confidence level (i.e.  ${\rm S/N_{\mu}} = \mu/\mu_{\rm err} < 2$ ). Finally, we identify the counterpart to each source in the Sloan Digital Sky Survey (SDSS) and require that all *Gaia* sources have morphologies consistent with being point sources (class = 6 in the SDSS) to limit our search to quasars only (i.e. excluding Seyferts and potential contaminating extended galaxies). This results in about 2% of the sample being removed due to extended morphology. Matching the *Gaia* sample to the SDSS with a matching radius of less than 1 arcsec also allows us to investigate the properties of our sample in optical colour-colour space.

In total, we find that there are 2,634 spatially unresolved Gaia sources with proper motions and 18 < G < 20 mag within one degree of the NGP, of which 100 sources ( $\approx 4\%$ ) have proper motions consistent with zero (within  $2\sigma$ ). These are shown as the blue circles in Fig. 1. Cross-matching our extracted catalogue with the SDSS data release 14 quasar sample (SDSS-DR14Q, Pâris et al. 2017) and the NASA/IPAC Extragalactic Database (NED) we find that 34 quasars are already spectroscopically confirmed within the same magnitude limit and region on the sky, of which 32 ( $\approx 95\%$ ) also have S/N<sub>u</sub> =  $\mu/\mu_{\rm err}$  < 2. For the remaining two the measured proper motions are  $2.76 \pm 1.09$  and  $1.22 \pm 0.58$  mas yr<sup>-1</sup>. We also discover two spectroscopically confirmed stars, observed as part of the SDSS-APOGEE survey (Alam et al. 2015). An extract of the full sample of Gaia sources with zero proper motions is presented in Table 1. We also examine the additional requirement that the sources have parallaxes consistent with zero within  $3\sigma$ , but only five sources (GQs 1255+2707, 1248+2658, 1247+2655, 1247+2706, and 1251+2804) were outside this criterion so we chose to include them for completeness.

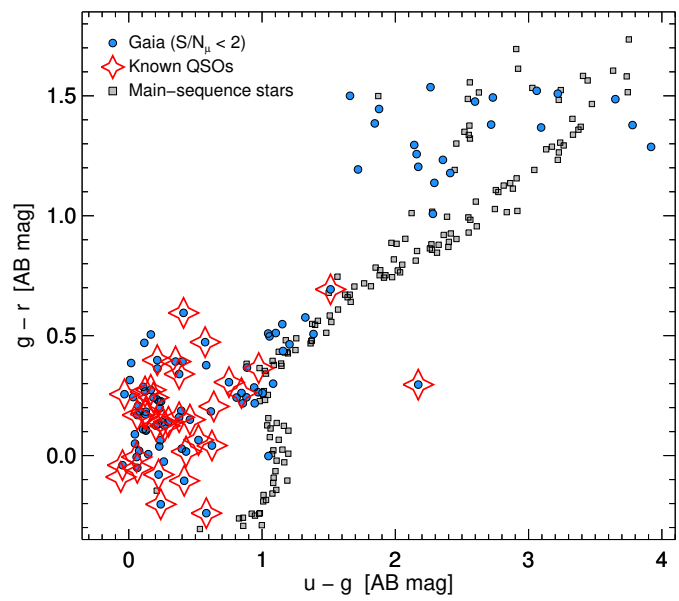


**Fig. 2.** Optical colour-colour plots of the *WISE*-detected Gaia point sources with proper motions and 18 < G < 20 mag (black dots) within one degree of the NGP. *Gaia* point sources with zero proper motions are represented by the blue dots and the spectroscopically confirmed quasars are shown by the red star symbols. Typical stellar colours are shown as grey dots.

### 3. Selection efficiency and completeness

We now investigate the location of the *Gaia* sources with zero proper motions in optical colour-colour space. By doing so, we can examine whether these candidate quasars have, e.g., ultraviolet excess typical of unobscured, low-z quasars (e.g. Sandage 1965; Schmidt & Green 1983). About 70% of the zero proper motion sources have blue (u - g < 1) colours (see Fig. 2). For quasars at  $z \gtrsim 2.2$ , the Lyman- $\alpha$  emission line will move out of the *u*-band, such that the quasars appear redder in u - g colour space. At red g - r colours (g - r > 1) the zero proper motion sources have optical colours consistent with M or G dwarf stars. While some of these are likely to be stellar contaminations, removing these candidates will also exclude dust-reddened quasars and broad absorption line (BAL) quasars from the sample, which are found to have very red optical colours and to be systematically missing in most existing quasar samples (Fynbo et al. 2013; Krogager et al. 2015; Ross et al. 2015; Krawczyk et al. 2015; Krogager et al. 2016).

To assess the efficiency of our selection we cross-match our sample of Gaia sources with zero proper motions to the allsky mid-infrared survey based on the WISE satellite (AllWISE; Wright et al. 2010). Mid-infrared selection of quasars is efficient at separating stars and galaxies from quasars and is not affected by dust extinction while also being sensitive to highredshift quasars. Of the 100 Gaia point sources with zero proper motions, we identify 76 of the counterparts in the AllWISE catalogue within 1 arcsec. This cross-match might introduce a bias excluding quasars with weak infrared emission. Stellar contaminants will also have weak infrared emission, however, and we find that of the 24 sources excluded in this approach, roughly half have a significant ultraviolet excess whereas the other half have optical colours consistent with the main-sequence stellar track. In Fig. 3 we show the zero proper motion *Gaia* sources in mid-infrared colour-colour space. Overplotted are contours of

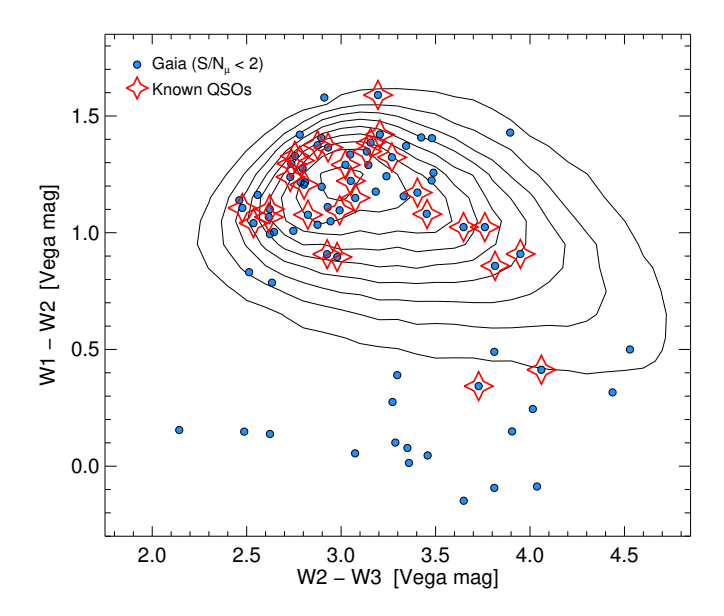


**Fig. 3.** *WISE* colour-colour plot of *Gaia* point sources with zero proper motions (blue dots) and SDSS DR14 quasars (red star symbols) within one degree of the NGP. Overplotted are contours of the full SDSS-DR14 quasar sample with mid-infrared counterparts in the AllWISE catalogue.

the SDSS-DR14Q sample for which WISE photometry exists. A simple color criterion of W1 - W2 > 0.8 has been found to be robust in identifying quasars at most redshifts (Stern et al. 2012). In our sample of zero proper motion sources with WISE photometry, 55 (70%) have W1 - W2 > 0.8 (of which 29 are already identified quasars). We consider the remaining 26 sources as high-likelihood quasars. All these have also been photometrically identifed as quasars by (Richards et al. 2009), and we list their estimated photometric redshifts in Table 1 as well, marked by a "P". We note, however, that at W1 - W2 < 0.8, two spectroscopically confirmed quasars have also been observed, one being a high-z quasar with optical colours consistent with known quasars in this redshift range and the other being a typical UV-excess quasar. We therefore consider the sources with zero proper motions and W1 - W2 < 0.8 as possible contaminants (excluding the two already known quasars). We then infer a conservative selection efficiency of  $N_{\rm QSO}/N_{\rm star} \gtrsim 75\%$ . This is a lower limit due to the population of quasars with blue W1-W2colours that also populates our sample.

We present our main result in Fig. 4 where we show the full sample of *Gaia* sources with 18 < G < 20 mag and within one degree of the NGP for which a counterpart in the AllWISE catalogue could be identified. It is clear from the figure that the majority of point sources selected on the basis of zero proper motions occupy a distinct region in  $S/N_{\mu} - WISE$  colour parameter space. This demonstrates that selecting quasars as stationary sources on the sky is definitely feasible and has a high efficiency of  $\gtrsim 75\%$ . The completeness is close to 100% within the defined magnitude limit, since all cosmological objects are selected without any prior assumptions on the spectral energy distributions.

#### 4. Discussion and conclusions

We have here demonstrated the possibility to select quasars as stationary objects in the *Gaia* DR2 data set. When observing fields well away from the Galactic stellar disk (here the NGP)

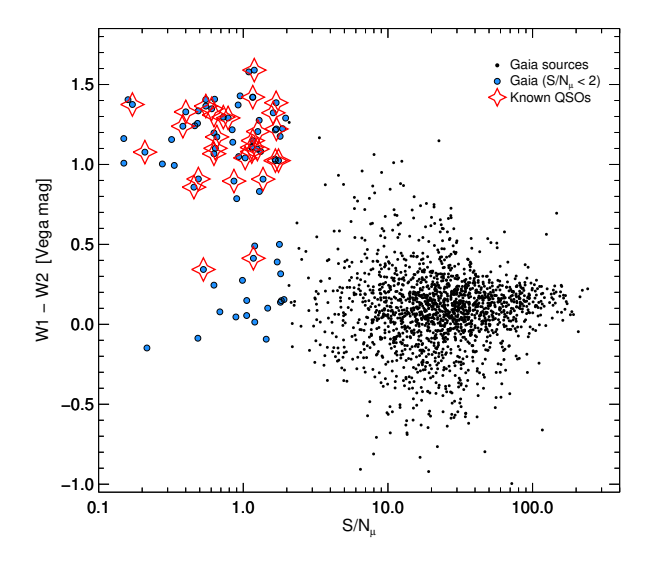


**Fig. 4.** W1-W2 colour as a function of S/N $_{\mu}$  of the WISE-detected Gaia point sources with proper motions and 18 < G < 20 mag (black dots) within one degree of the NGP. Gaia point sources with zero proper motions are represented by blue dots and spectroscopically confirmed quasars are shown with red star symbols.

the contamination from stars is very modest (below 25%) when targeting the most relevant magnitudes (here 18 < G < 20). Hence, astrometric selection offers both a complete and clean selection of quasars.

This technique offers the possibility to take major steps ahead on some very interesting problems relating to the quasar phenomenon. We will mention a few examples here. First, getting a more complete picture of dust obscuration in quasar hosts will be possible with a sample of quasars selected from proper motion. Second, the redshift dependence of the frequency of BAL quasars can be determined. Third, using a purely astrometrically selected sample of quasars we can get an independent gauge of the metallicity distribution of intervening galaxies, in particular the damped Lyman- $\alpha$  absorbers. Fourth, the identification of quasars via zero proper motion also provides unbiased measures of number densities of various absorbers, such as Civ, Mg II, or H I. Such a sample will still be subject to a flux limit, but this is easier to model than the combined effect of a flux limit and the effect of dust reddening on the quasar selection efficiency in optical quasar surveys. We also note that the Gaia DR2 data have been applied to find new gravitationally lensed quasars (Krone-Martins et al. 2018).

An interesting case is the confirmed quasar SDSS J125209.59+265018.4 (GQ125209+265018 in Table 1). In Fig. 2 this is located as the object on the stellar track at u - g = 1.5. In Fig. 3 it is one of the two sources with blue WISE colours at W1 - W2 < 0.8. This illustrates well the potential of selection of quasars from astrometry in finding quasars that are otherwise difficult to photometrically identify.

When the full *Gaia* data is released, the errors on the proper motions will decrease and it will thus be easier to disentangle objects that are truly stationary (quasars) and stars with low proper motions. This will also make it possible to search for stationary sources at even fainter magnitudes. Also, since Gaia astrometry exists for most of the sky, this proper motion criteria could help reduce the contamination in other quasar surveys. Since Gaia covers the full sky, the selection can also be carried out for a large sample of sources – however, with the caveat that the contamination from apparently stationary stars increases sig-

nificantly closer to the Galactic plane. We can also estimate the expected contamination of e.g. the WISE W1-W2 color selection, where it can be seen from Fig. 4 that 15% of the sources with W1-W2>0.8 have significant proper motions at more than  $5\sigma$ .

*Acknowledgements.* KEH and PJ acknowledge support by a Project Grant (162948–051) from The Icelandic Research Fund. The Cosmic Dawn Center is funded by the DNRF. LC is supported by DFF – 4090-00079.

#### References

Sandage, A. 1965, ApJ, 141, 1560

Schmidt, M. & Green, R. F. 1983, ApJ, 269, 352

Schneider, D. P., Richards, G. T., Hall, P. B., et al. 2010, AJ, 139, 2360 Secrest, N. J., Dudik, R. P., Dorland, B. N., et al. 2015, ApJS, 221, 12 Stern, D., Assef, R. J., Benford, D. J., et al. 2012, ApJ, 753, 30 Weymann, R. J., Carswell, R. F., & Smith, M. G. 1981, ARA&A, 19, 41 Wright, E. L., Eisenhardt, P. R. M., Mainzer, A. K., et al. 2010, AJ, 140, 1868

Alam, S., Albareti, F. D., Allende Prieto, C., et al. 2015, ApJS, 219, 12 Brusa, M., Civano, F., Comastri, A., et al. 2010, ApJ, 716, 348 Crampton, D., Cowley, A. P., & Hartwick, F. D. A. 1987, ApJ, 314, 129 Fynbo, J. P. U., Krogager, J.-K., Venemans, B., et al. 2013, ApJS, 204, 6 Gaia Collaboration, Brown, A. G. A., Vallenari, A., et al. 2018, ArXiv e-prints [arXiv:1804.09365] Heintz, K. E., Fynbo, J. P. U., & Høg, E. 2015, A&A, 578, A91 Hewett, P. C. & Foltz, C. B. 1994, PASP, 106, 113 Ivezić, Ž., Menou, K., Knapp, G. R., et al. 2002, AJ, 124, 2364 Krawczyk, C. M., Richards, G. T., Gallagher, S. C., et al. 2015, AJ, 149, 203 Krogager, J.-K., Fynbo, J. P. U., Heintz, K. E., et al. 2016, ApJ, 832, 49 Krogager, J.-K., Geier, S., Fynbo, J. P. U., et al. 2015, ApJS, 217, 5 Krone-Martins, A., Delchambre, L., Wertz, O., et al. 2018, ArXiv e-prints [arXiv:1804.11051] Lindegren, L., Hernandez, J., Bombrun, A., et al. 2018, ArXiv e-prints [arXiv:1804.09366] Maddox, N., Hewett, P. C., Péroux, C., Nestor, D. B., & Wisotzki, L. 2012, MN-RAS, 424, 2876 Pâris, I., Petitjean, P., Aubourg, E., et al. 2017, ArXiv e-prints [arXiv:1712.05029] Richards, G. T., Myers, A. D., Gray, A. G., et al. 2009, ApJS, 180, 67 Ross, N. P., Hamann, F., Zakamska, N. L., et al. 2015, MNRAS, 453, 3932

**Table 1.** Point sources within one degree of the NGP with proper motions consistent with zero (within  $2\sigma$ ) and 18 < G < 20 mag.

Source	R.A.	Decl.	и	g	r	i	Z	W1 - W2	$z_{\rm QSO}$
GQ125420+274609	12:54:20.0	+27:46:09.6	23.2	21.4	20.0	19.1	18.7	-	-
GQ125302+261711	12:53:02.1	+26:17:11.2	20.0	19.4	19.6	19.5	19.2	0.86	2.32
GQ125358+262453	12:53:58.1	+26:24:53.7	20.9	20.1	19.8	19.9	19.8	0.91	3.10
GQ125302+262722	12:53:02.2	+26:27:22.5	19.7	19.5	19.1	19.0	19.1	1.21	1.26
GQ125456+263623	12:54:56.8	+26:36:23.8	23.2	20.8	19.6	19.0	18.8	-0.09	_
GQ125510+263724	12:55:10.1	+26:37:25.0	21.0	20.2	19.9	19.9	19.8	-	_
GQ125424+263941	12:54:24.3	+26:39:41.8	19.3	19.1	19.2	19.0	19.1	1.59	1.60
GQ125453+263721	12:54:53.0	+26:37:21.8	20.9	19.8	19.5	19.4	19.2	-	-
GQ125503+264502	12:55:03.8	+26:45:02.7	21.3	20.2	19.6	19.4	19.2	_	_
GQ125441+264637	12:54:41.3	+26:46:37.8	20.9	19.7	19.3	19.0	19.0	_	_
GQ125424+264833	12:54:24.6	+26:48:33.8	20.1	19.9	19.7	19.6	19.7	1.22	1.47P
GQ125424+264653 GQ125516+265049	12:55:16.1	+26:50:49.0	25.0	21.1	19.7	19.0	18.9	-	1.4/1
			23.9	21.1	19.8	18.2	17.5	0.16	-
GQ125518+270034	12:55:18.6	+27:00:34.3							-
GQ125543+270714	12:55:43.7	+27:07:14.1	23.8	21.0	19.7	18.2	17.5	0.14	star
GQ125126+261346	12:51:26.6	+26:13:46.9	19.6	19.7	19.4	19.3	19.4	1.11	1.43
GQ124943+261629	12:49:43.8	+26:16:29.7	18.9	18.9	18.7	18.5	18.5	0.34	1.84
GQ124959+261949	12:49:59.0	+26:19:49.3	21.1	20.2	19.9	19.7	19.7	-	-
GQ125031+261953	12:50:31.6	+26:19:53.7	19.6	19.4	19.3	19.4	19.4	1.00	0.88P
GQ125027+263048	12:50:27.3	+26:30:48.1	20.7	19.5	19.0	18.8	18.7	-	-
GQ125248+263805	12:52:48.3	+26:38:05.6	24.8	21.6	20.1	19.0	18.3	0.08	-
GQ125150+263900	12:51:50.7	+26:39:00.1	17.7	17.6	17.4	17.2	17.1	0.90	1.91
GQ125133+264550	12:51:33.7	+26:45:50.4	20.0	19.9	19.4	19.4	19.5	1.42	1.28P
GQ125209+265018	12:52:09.6	+26:50:18.5	21.9	20.4	19.7	19.5	19.3	0.41	3.44
GQ124902+262014	12:49:02.2	+26:20:14.7	22.6	20.8	19.7	19.1	18.8	-	-
GQ125008+263658	12:50:09.0	+26:36:58.6	19.7	19.3	19.3	19.2	19.2	1.05	0.68P
GQ124835+263759	12:48:35.0	+26:37:59.8	20.1	20.1	19.9	19.8	19.9	1.28	1.15P
GQ124820+264225	12:48:20.6	+26:42:25.1	20.4	19.4	19.4	19.4	19.6	-	-
GQ124926+264101	12:49:26.1	+26:41:01.4	19.7	19.3	19.2	19.2	19.2	1.10	0.67
GQ124921+264446	12:49:21.2	+26:44:46.8	19.9	19.9	19.6	19.6	18.9	0.99	0.31P
GQ125054+264353	12:50:55.0	+26:43:53.6	20.1	19.8	19.6	19.2	19.2	1.22	1.59P
GQ125015+264337	12:50:16.0	+26:43:37.6	18.5	18.4	18.4	18.2	18.3	1.38	1.79
GQ125149+265349	12:51:49.2	+26:53:50.0	23.1	21.0	19.8	19.3	19.1	0.50	star
GQ124945+264953	12:49:45.5	+26:49:53.3	25.0	21.2	19.8	19.1	18.8	0.25	-
GQ124941+265314	12:49:41.0	+26:53:14.8	20.5	19.9	19.7	19.7	19.6	-	2.46P
GQ125023+265328	12:50:23.6	+26:53:28.7	19.8	19.4	19.0	18.9	18.9	1.08	1.49
GQ124935+265906	12:49:35.2	+26:59:06.4	25.0	21.4	19.9	19.1	18.7	0.15	-
GQ125006+265939	12:50:06.3	+26:59:39.9	19.9	19.8	19.5	19.7	19.7	1.20	0.97
GQ125421+265454	12:54:21.0	+26:54:54.7	20.2	20.0	19.6	19.6	19.6	1.16	1.30P
GQ125429+270003	12:54:29.8	+27:00:03.8	19.7	19.5	19.4	19.1	19.2	1.10	1.64
GQ125429+270005 GQ125312+265355	12:53:12.1	+26:53:55.7	24.6	21.5	20.0	18.9	18.4	-	-
GQ125312+205555 GQ125302+270519	12:53:12.1	+27:05:19.9	22.6	20.4	20.0	20.0	20.0	1.02	2.99
GQ125302+270519 GQ125320+270607	12:53:20.1	+27:06:07.4	20.1	19.7	19.1	18.8	18.9	1.32	1.15
GQ125528+271330	12:55:28.8	+27:13:30.1	20.0	19.8	19.5	19.7	19.7	1.30	1.03
GQ125357+271630	12:53:57.5	+27:16:30.6	22.2	19.9	18.9	18.5	18.3	- 1 50	- 0.00D
GQ125359+272014	12:53:59.8	+27:20:14.8	20.6	20.3	20.3	19.9	20.4	1.58	0.08P
GQ125158+271304	12:51:58.6	+27:13:04.1	21.6	20.2	19.7	19.5	19.6	1 42	1 40
GQ125300+271234	12:53:00.1	+27:12:34.2	19.5	19.2	19.1	19.0	19.0	1.42	1.48
GQ125241+272550	12:52:41.1	+27:25:50.8	21.4	21.2	20.7	20.1	19.9	1.22	0.22P
GQ125134+272000	12:51:34.4	+27:20:00.2	20.9	19.9	19.7	19.7	19.7	-	-
GQ125107+271451	12:51:08.0	+27:14:51.5	20.2	19.8	19.4	19.2	18.8	0.79	0.38P
GQ125206+272717	12:52:07.0	+27:27:17.5	18.7	18.6	18.6	18.4	18.5	1.22	1.68
GQ125211+272803	12:52:11.9	+27:28:03.8	20.7	20.6	20.4	20.0	20.1	1.41	1.87P
GQ125332+272225	12:53:32.1	+27:22:25.1	19.6	19.3	19.2	18.9	18.8	1.39	1.63
GQ125320+272116	12:53:20.3	+27:21:16.0	18.0	17.8	18.0	17.9	17.8	1.04	0.51
GQ125353+273405	12:53:53.7	+27:34:05.9	21.4	20.3	19.8	19.5	19.5	0.39	-
GQ125308+273331	12:53:08.5	+27:33:31.2	23.8	21.6	20.4	19.2	18.5	-0.09	-
GQ125327+273733	12:53:27.1	+27:37:33.1	19.9	19.9	19.8	19.6	19.4	1.08	1.96P
GQ125257+274542	12:52:58.0	+27:45:42.5	19.0	18.7	18.6	18.5	18.4	1.32	2.00
GQ124816+264712	12:48:16.3	+26:47:12.3	18.1	18.1	18.2	17.9	17.8	1.35	1.86
GQ124746+264709	12:47:46.5	+26:47:09.8	21.2	20.2	20.0	19.8	19.7	-	-
GQ124816+265235	12:48:16.4	+26:52:35.3	20.1	19.5	19.4	19.4	19.3	-	2.51
-									

Table 1. continued.

Source	R.A.	Decl.	и	g	r	i	z	W1 - W2	Z <sub>QSO</sub>
GQ124832+265312	12:48:32.8	+26:53:12.7	18.2	17.8	17.9	17.7	17.8	1.11	0.59
GQ124804+265836	12:48:05.0	+26:58:36.1	24.8	22.2	20.7	19.1	18.3	0.15	-
GQ124715+265528	12:47:15.9	+26:55:28.1	22.4	20.1	18.9	18.6	18.3	-	-
GQ124721+265728	12:47:21.3	+26:57:28.9	21.3	20.2	19.7	19.5	19.4	-	-
GQ124725+270114	12:47:25.8	+27:01:14.1	19.8	19.3	19.2	19.2	19.0	1.07	0.80
GQ124731+270622	12:47:31.5	+27:06:22.2	20.9	20.0	19.8	19.7	19.8	-	-
GQ124734+270615	12:47:34.4	+27:06:15.2	23.7	21.8	20.3	19.0	18.3	0.05	-
GQ124922+265938	12:49:22.2	+26:59:38.9	21.3	20.1	19.7	19.5	19.5	-	-
GQ124955+271335	12:49:55.7	+27:13:35.3	19.5	19.4	19.3	19.2	19.2	1.37	1.47P
GQ124846+271722	12:48:46.1	+27:17:22.7	19.8	19.4	19.1	18.8	18.7	1.29	1.51
GQ124814+271603	12:48:14.5	+27:16:03.6	22.8	20.4	19.2	18.6	18.3	-0.15	-
GQ124809+271650	12:48:09.4	+27:16:50.1	20.2	20.0	19.7	19.8	19.7	1.16	0.95P
GQ124925+272634	12:49:26.0	+27:26:34.5	18.7	18.5	18.3	18.4	18.5	1.37	1.16
GQ124728+272742	12:47:28.6	+27:27:42.5	21.2	20.7	20.3	19.9	19.9	-	0.46P
GQ124752+273018	12:47:52.3	+27:30:18.9	20.4	20.0	19.9	19.9	19.8	0.91	0.91
GQ125043+271934	12:50:44.0	+27:19:34.3	20.3	20.2	20.1	20.2	20.0	0.83	0.93P
GQ125050+272448	12:50:50.2	+27:24:48.4	24.6	21.5	20.1	18.7	17.9	0.06	-
GQ125039+272904	12:50:39.4	+27:29:04.4	20.7	20.1	19.6	19.1	18.9	1.15	1.89
GQ125104+273341	12:51:04.1	+27:33:41.2	20.2	20.2	19.8	19.8	20.1	1.24	1.15P
GQ124958+273317	12:49:58.2	+27:33:17.5	20.0	19.8	19.8	19.7	19.6	1.26	1.72P
GQ125013+273256	12:50:13.7	+27:32:56.4	19.9	19.8	19.6	19.5	19.7	1.14	1.15P
GQ125008+274001	12:50:08.6	+27:40:01.5	21.1	20.1	19.9	19.7	19.8	0.32	-
GQ125042+274012	12:50:42.4	+27:40:13.0	20.2	20.0	19.7	19.6	19.6	1.41	1.48P
GQ125033+274519	12:50:33.6	+27:45:19.1	20.0	19.8	19.7	19.6	19.7	1.41	1.48P
GQ125019+274443	12:50:19.2	+27:44:43.1	20.5	19.7	19.4	19.1	18.7	1.02	2.67
GQ125007+274709	12:50:07.9	+27:47:09.4	23.6	21.4	19.8	18.7	18.0	0.28	-
GQ125202+275018	12:52:02.1	+27:50:18.6	19.3	18.8	18.7	18.7	18.5	1.17	2.48
GQ125312+275524	12:53:12.1	+27:55:24.6	19.7	19.5	19.3	19.3	19.2	1.18	1.00P
GQ125230+275410	12:52:30.1	+27:54:10.0	19.4	19.3	19.0	19.1	19.1	1.03	1.04P
GQ125241+275942	12:52:42.0	+27:59:42.7	24.0	21.8	20.6	19.1	18.3	0.10	-
GQ125239+280127	12:52:39.2	+28:01:27.2	19.6	19.6	19.5	19.4	19.2	1.29	2.04P
GQ125249+280356	12:52:49.1	+28:03:56.4	19.4	19.3	19.2	19.4	19.2	1.01	0.93P
GQ125112+275222	12:51:12.3	+27:52:22.4	19.0	18.8	18.5	18.5	18.6	1.24	1.04
GQ125159+280446	12:51:59.1	+28:04:46.3	23.1	21.4	19.9	18.8	18.2	0.01	-
GQ124901+274330	12:49:01.8	+27:43:30.2	21.1	20.2	19.8	19.7	19.5	-	-
GQ124915+274554	12:49:15.9	+27:45:54.8	19.6	19.3	19.3	19.2	18.9	1.43	2.16P
GQ124955+275657	12:49:55.4	+27:56:57.7	21.2	19.9	19.3	19.0	18.9	0.49	-
GQ124958+275703	12:49:58.1	+27:57:03.7	19.8	19.6	19.4	19.1	19.0	1.34	1.91P
GQ125005+280041	12:50:05.2	+28:00:41.9	21.0	20.2	20.0	19.8	19.7	-	

**Notes.** Right ascension and declination are from the *Gaia* DR2 catalogue. Optical magnitudes are in the AB system and are from the SDSS photometric data. The mid-infrared W1-W2 colours are from the AllWISE catalogue and are in the Vega system. Spectroscopic redshifts are based on the already identified quasars in the SDSS-DR14 quasar survey (Pâris et al. 2017) or the NED database (specifically from Crampton et al. 1987). Photometric redshifts (marked by a "P") are from Richards et al. (2009).

## Appendix A: Thumbnail images of all sources

Thumbnails of all point sources within one degree of the NGP with proper motions consistent with zero (within  $2\sigma$ ) and 18 < G < 20 mag.

GQ124715+265528	GQ124721+265728	GQ124725+270114 z <sub>oso</sub> =0.80	GQ124728+272742 Z <sub>phot</sub> =0.46	GQ124731+270622
•		•	<b>a</b>	
1.				
10 arcsec	10 arcsec	10 arcsec	10 arcsec	10 arcsec
GQ124734+270615	GQ124746+264709	GQ124752+273018 z <sub>QSO</sub> =0.91	GQ124804+265836	GQ124809+271650 z <sub>phot</sub> =0.95
				•
10 arcsec	10 arcsec	10 arcsec	10 arcsec	10 arcsec
GQ124814+271603	GQ124816+264712 z <sub>QSO</sub> =1.86	GQ124816+265235 z <sub>QSO</sub> =2.51	GQ124820+264225	GQ124832+265312 z <sub>QSO</sub> =0.59
*	•			
* * *				
	*			***
10 arcsec	10 arcsec	10 arcsec	10 arcsec	10 arcsec
GQ124835+263759 z <sub>phoi</sub> =1.15	GQ124846+271722 z <sub>OSO</sub> =1.51	GQ124901+274330	GQ124902+262014	GQ124915+274554 z <sub>phot</sub> =2.16
1				
10 arcsec	10 arcsec	10 arcsec	10 arcsec	10 arcsec
GQ124921+264446 z <sub>phot</sub> =0.31	GQ124922+265938	GQ124925+272634 z <sub>QSO</sub> =1.16	GQ124926+264101 z <sub>QSO</sub> =0.67	GQ124935+265906
		•	•	
				* 7
10 arcsec	10 arcsec	10 arcsec	10 arcsec	10 arcsec
GQ124941+265314 z <sub>phol</sub> =2.46	GQ124943+261629 z <sub>OSO</sub> =1.84	GQ124945+264953	GQ124955+271335 z <sub>phot</sub> =1.47	GQ124955+275657
				1 1 1 1 1 1 1 1 1 1 1 1 1 1 1 1 1 1 1
10 arcsec	10 arcsec	10 arcsec	10 arcsec	10 arcsec

**Fig. A.1.**  $50 \times 50$  arcsec<sup>2</sup> thumbnails around each stationary source.

GQ124958+273317 z <sub>phot</sub> =1.72	GQ124958+275703 Z <sub>phot</sub> =1.91	GQ124959+261949	GQ125005+280041	GQ125006+265939 z <sub>OSO</sub> =0.97
10 arcsec				
GQ125007+274709	GQ125008+263658	GQ125008+274001	GQ125013+273256	GQ125015+264337
	z <sub>phot</sub> =0.68	GQ123000+274001	Z <sub>phot</sub> =1.15	z <sub>oso</sub> =1.79
	. *	**		
•				
10 arcsec				
GQ125019+274443	GQ125023+265328	GQ125027+263048	GQ125031+261953	GQ125033+274519
z <sub>QSO</sub> =2.67	z <sub>oso</sub> =1.49		z <sub>phot</sub> =0.88	Z <sub>phot</sub> =1.48
10 arcsec				
GQ125039+272904 z <sub>OSO</sub> =1.89	GQ125042+274012 z <sub>phol</sub> =1.48	GQ125043+271934 z <sub>phot</sub> =0.93	GQ125050+272448	GQ125054+264353 z <sub>phot</sub> =1.59
10 arcsec				
GQ125104+273341 z <sub>phot</sub> =1.15	GQ125107+271451 z <sub>phot</sub> =0.38	GQ125112+275222 z <sub>oso</sub> =1.04	GQ125126+261346 z <sub>QSO</sub> =1.43	GQ125133+264550 z <sub>phot</sub> =1.28
-pnot · · · · · ·	- pnot	-450	-450	=pnot ==
10 arcsec				
GQ125134+272000	GQ125149+265349	GQ125150+263900	GQ125158+271304	GQ125159+280446
		z <sub>QSO</sub> =1.91		
		•		
10 arcsec				
GQ125202+275018 z <sub>QSO</sub> =2.48	GQ125206+272717 z <sub>QSO</sub> =1.68	GQ125209+265018 z <sub>QSO</sub> =3.44	GQ125211+272803 z <sub>phot</sub> =1.87	GQ125230+275410 z <sub>phot</sub> =1.04
• *	•		Learner and Comment	
10 arcsec				
. <del> </del>				

**Fig. A.2.**  $50\times50~\rm arcsec^2$  thumbnails around each stationary source. Article number, page 8 of 9

GQ125239+280127 z <sub>phot</sub> =2.04	GQ125241+272550 z <sub>phot</sub> =0.22	GQ125241+275942	GQ125248+263805	GQ125249+280356 z <sub>phot</sub> =0.93
10 arcsec	10 arcsec	10 arcsec	10 arcsec	10 arcsec
GQ125257+274542 z <sub>QSO</sub> =2.00	GQ125300+271234 z <sub>oso</sub> =1.48	GQ125302+261711 z <sub>oso</sub> =2.32	GQ125302+262722 z <sub>oso</sub> =1.26	GQ125302+270519 z <sub>oso</sub> =2.99
10 arcsec	10 arcsec	10 arcsec	10 arcsec	10 arcsec
GQ125308+273331	GQ125312+265355	GQ125312+275524	GQ125320+270607	GQ125320+272116
		z <sub>phot</sub> =1.00	z <sub>QSO</sub> =1.15	z <sub>oso</sub> =0.51
10 arcsec	10 arcsec	10 arcsec	10 arcsec	10 arcsec
GQ125327+273733 z <sub>phot</sub> =1.96	GQ125332+272225 z <sub>QSO</sub> =1.63	GQ125353+273405	GQ125357+271630	GQ125358+262453 z <sub>QSO</sub> =3.10
to an age				
	•			
10 arcsec	10 arcsec	10 arcsec	10 arcsec	10 arcsec
GQ125359+272014 z <sub>phot</sub> =0.08	GQ125420+274609	GQ125421+265454 z <sub>phot</sub> =1.30	GQ125424+263941 z <sub>QSO</sub> =1.60	GQ125424+264833 Z <sub>phot</sub> =1.47
4.			•	
•				
10 arcsec	10 arcsec	10 arcsec	10 arcsec	10 arcsec
GQ125429+270003	GQ125441+264637	GQ125453+263721	GQ125456+263623	GQ125503+264502
z <sub>QSO</sub> =1.64				
				*
10 arcsec	10 arcsec	10 arcsec	10 arcsec	10 arcsec
GQ125510+263724	GQ125516+265049	GQ125518+270034	GQ125528+271330	GQ125543+270714
			z <sub>QSO</sub> =1.03	
	* *			

Fig. A.3.  $50 \times 50$  arcsec<sup>2</sup> thumbnails around each stationary source.